On Ohmic heating in the Earth's core I

Nutation constraints

Author(s):
Jackson, Andrew; Livermore, Philip

Publication date:
2009

Permanent link:
https://doi.org/10.3929/ethz-b-000013242

Originally published in:
Geophysical Journal International 177(2), https://doi.org/10.1111/j.1365-246X.2008.04008.x

Geophys. J. Int. (2009) **177,** 367–382 doi: 10.1111/j.1365-246X.2008.04008.x

On Ohmic heating in the Earth's core I: nutation constraints

Andrew Jackson[1] and Philip Livermore[2]

[1]*Institute for Geophysics, ETH Zürich,* CH-8093 *Switzerland. E-mail: ajackson@ethz.ch*
[2]*IGPP, Scripps Institution of Oceanography, UCSD, La Jolla,* CA 92093, *USA*

Accepted 2008 October 2. Received 2008 October 1; in original form 2008 May 14

SUMMARY

We present calculations to place formal lower bounds on the energy dissipated by the magnetic field in the core. These bounds are discovered by solving for 3-D magnetic fields in the Earth's core that are optimally configured for minimizing the dissipation. Such bounds are relevant for addressing the balance of heat flow through the core–mantle boundary into the mantle, and thus for constraining Earth's history scenarios. The bounds we derive are based on a number of different constraints. We use observed values of the magnetic field at the core–mantle boundary for epoch 2001, and also the root-mean-square values of the radial magnetic field on the inner core boundary and the core mantle boundary inferred from interpretations of the Earth's nutations. A formal lower bound for the dissipation based on all the constraints is almost 10 GW. This lower bound is achieved for a 3-D magnetic field configuration that has very unlikely features. We present two further geophysically reasonable (but no longer rigorous) calculations that raise the dissipation towards 100 GW, not dissimilar to other recent estimates of dissipation.

Key words: Electromagnetic theory; Dynamo: theories and simulations; Heat flow.

1 INTRODUCTION

There is currently considerable interest in the heat budget of the Earth, and in particular, in quantifying the contribution of the core to the total budget. On the one hand, the amount of heat leaving the core is important in governing the process of mantle convection, since convection with a significant heating from below can be different in character to primarily internally heated convection (Schubert *et al.* 2001). On the other hand, the amount of heat flowing through the core–mantle boundary (CMB) is intimately related to the heat needed to drive the geodynamo and maintain the magnetic field through time. This quantity is central to studies of convection in the core, with interesting repercussions for the entire evolution of the Earth; indeed, the age of the inner core (since formation) hinges crucially on this quantity (e.g. Nimmo 2007). Several lines of argument are available for estimating the partitioning of heat flow, but it is remarkable how large the range of possibilities is for the heat leaving the core, with probably an order of magnitude of difference between lower and upper values.

Of the 44 TW of heat leaving the Earth (Chapman & Pollack 1975), perhaps 20 TW is thought to be generated in the mantle from radioactivity if we adopt the CI chondrite model of McDonough & Sun (1995), which contains 240 ppm of potassium. In addition, a further 8 TW is generated in the crust. The remaining mantle contribution we should account for is the heat lost through cooling. This is difficult to estimate and leads to perhaps 7–15 TW of heat. The core contribution is clearly very poorly defined under this accounting, clearly between 1 and 9 TW, in other words an order of magnitude of uncertainty. Lay *et al.* (2008) have reviewed the situation and give similar figures, though some have even larger uncertainties than those we give.

A new method for estimating the temperature gradient at the base of the mantle, and hence the heat flow, has emerged as a result of the discovery of the post-perovskite transition close to the CMB (Iitaka *et al.* 2004; Murakami *et al.* 2004; Oganov & Ono 2004). In this method, a double-crossing of the perovskite to post-perovskite transition can occur as a result of the strong temperature gradient in the thermal boundary layer at the base of the mantle. The thermal conductivity of the mantle is required to perform the conversion, and indeed there is controversy over the value of this figure for mantle materials; disregarding this for the moment, the value for the heat flux at the base of the mantle is in the range 9–13 TW according to the studies of Hernlund *et al.* (2005) and 9–17 TW according to Lay *et al.* (2006).

A lower bound on the heat leaving the core is simply the heat flowing down the adiabat at the CMB, though this depends on the assumption that the whole of the core is well mixed; a stably stratified layer at the top of the core could reduce this number. Recent estimates of the heat flowing down the adiabat vary, but the range 6–8 TW seems representative (Gubbins *et al.* 2003; Roberts *et al.* 2003). Arguments based on the heat flux carried by plumes originating at the CMB give estimates in the range of 3–9 TW (Montelli *et al.* 2004) or 2–3 TW (Davies 1999).

Another set of estimates for the heat leaving the core is based on thermodynamic arguments, and requires a figure for the entropy needed to drive the dynamo, sometimes loosely called the dissipation and given as an energy rather than an entropy. The dissipation is the amount of energy lost by Ohmic heating in the core due to its finite electrical conductivity. This figure has been estimated in several ways. If one adopts the view of Roberts *et al.* (2003), the dissipation takes a value 1–2 TW; similarly Gubbins *et al.* (2003) give the value of approximately 2 TW (equivalent to an entropy of $500\,\mathrm{MW\,K^{-1}}$), but the objectivity of the methods used to determine the entropy needed is somewhat wanting. The former originates with estimates of the spectrum of energy in the core and makes links with behaviour of dynamo models. The latter simply sets the Ohmic dissipation equal to the entropy increase due to thermal conduction down the adiabat. A separate recent estimate of Christensen & Tilgner (2004) is based on scaling the energetics of numerous numerical dynamo models to reach the relevant regime of the Earth, with corroboration of the scaling provided by the results of the Karlsruhe dynamo experiment (Stieglitz & Müller 2001). This gives estimates in the range 0.2–0.5 TW.

A few words are in order concerning the connection between the dissipation and the heat flow at the CMB. Because of thermodynamic efficiency constraints, the dissipation is only a fraction of the heat flow through the CMB. When convection is generated by latent heat and light element release at the inner core boundary (ICB), dissipations of 1–2 TW are associated with heat flows of perhaps 5–10 TW. In the absence of an inner core, these figures essentially double and there become grave difficulties with the driving mechanisms for the dynamo. Such a discussion is outside the scope of this paper, details can be found in, for example, Roberts *et al.* (2003).

Another approach, originating in the work of Parker (1972), places a rigorous lower bound on the Ohmic heating in the core (the dissipation referred to above) based purely on the observed values of the magnetic field. Parker asked the question, 'what is the minimum value of the mean-square current density (over the whole core) that could be associated with the observed value of the Earth's dipole field?'. He used variational calculus to show that there is a unique minimum value of this quantity compatible with the measured dipole field. If $\mathbf{J}$ is the current density and a value for the electrical conductivity of the core σ is supplied, then the Ohmic heating Φ can be duly calculated as

$$\Phi = \frac{1}{\sigma}\int \mathbf{J}^2\,\mathrm{d}V = \frac{1}{\mu_0^2\sigma}\int_V (\nabla\wedge\mathbf{B})^2\,\mathrm{d}V. \tag{1}$$

Here, we have used the Maxwell equation $\nabla\wedge\mathbf{B}=\mu_0\mathbf{J}$ to relate $\mathbf{J}$ to the magnetic field $\mathbf{B}$. Indeed, when a modern value for the dipole moment of $\mathbf{B}$ is used, (1) gives $\Phi = 5.7\times10^7$ W. Actually in the original paper, Parker turned the problem around and adopted a steady state assumption (that the heat emerging from the core cannot exceed that observed to be flowing out of the Earth's surface) to place a bound on the electrical conductivity of the core.

A significant refinement of Parker's calculation was provided by Gubbins (1975), who generalized the calculation to take into account all the harmonics of the observed magnetic field. We shall refer to this problem in the rest of the paper as the canonical P–G (i.e. Parker–Gubbins) problem. In what follows we take a to be the Earth's radius, c to be the core radius and b to be the inner core radius. The exterior magnetic field $\mathbf{B}$, measured in spherical polar coordinates (r,θ,ϕ), is represented as the gradient of a potential V as

$$\mathbf{B} = -\nabla V, \tag{2}$$

and V is expanded as a series of Schmidt quasi-normalized spherical harmonics with associated Gauss coefficients $\{g_l^m;h_l^m\}$ in the form

$$V = a\sum_{l,m}\left(\frac{a}{r}\right)^{l+1}\left[g_l^m\cos m\phi + h_l^m\sin m\phi\right]P_l^m(\cos\theta), \tag{3}$$

where P_l^m is an associated Legendre function. We shall find it convenient to write (3) in the compact form

$$V = a\sum_{l,m}\left(\frac{a}{r}\right)^{l+1}\beta_l^m Y_l^m(\theta,\phi), \tag{4}$$

where Y_l^m is a spherical harmonic and with an obvious identification of the coefficients $\{\beta_l^m\}$ with the Gauss coefficients $\{g_l^m;h_l^m\}$. The Y_l^m satisfy

$$\int \left(Y_l^m\right)^2\,\mathrm{d}\Omega = \left\langle\left(Y_l^m\right)^2\right\rangle = \frac{4\pi}{2l+1}, \tag{5}$$

where $\mathrm{d}\Omega$ is the element of solid angle on the surface of a sphere, and we have introduced the notation $\langle\,\rangle$, used frequently in the paper, to signify the integral over the sphere. We use $\langle\,\rangle_l$ to signify the contribution of degree l to $\langle\,\rangle$, and also refer in the paper to root-mean-square (rms) values over the sphere, for example, $B_r(c)_{\mathrm{rms}}$ is the rms value of B_r over radius c. The relation between the two notations is clearly $4\pi\,B_r(c)^2_{\mathrm{rms}} = \langle B_r(c)^2\rangle$.

When one uses the normalization of (5) together with (4), it transpires that the minimum Ohmic heating associated with the observed field can be written in the form

$$\Phi_{\min} = \frac{4\pi c}{\mu_0^2\sigma}\sum_{l,m}\frac{(l+1)(2l+1)(2l+3)}{l}\left(\frac{a}{c}\right)^{2l+4}\left(\beta_l^m\right)^2, \tag{6}$$

where μ_0 is the permeability of free space (Gubbins 1975); for an accessible treatment of the problem, see section 5.5 of Backus *et al.* (1996), though note the different normalizations employed therein. The observed values of the Gauss coefficients can be used out to degree 14, at which point it is well accepted that the crustal magnetic field begins to dominate (see Fig. 1). Using degrees l = 1–14 of the model CO2 (Holme *et al.* 2003) from the observations of the CHAMP satellite gives $\Phi = 2.93\times10^8$ W.

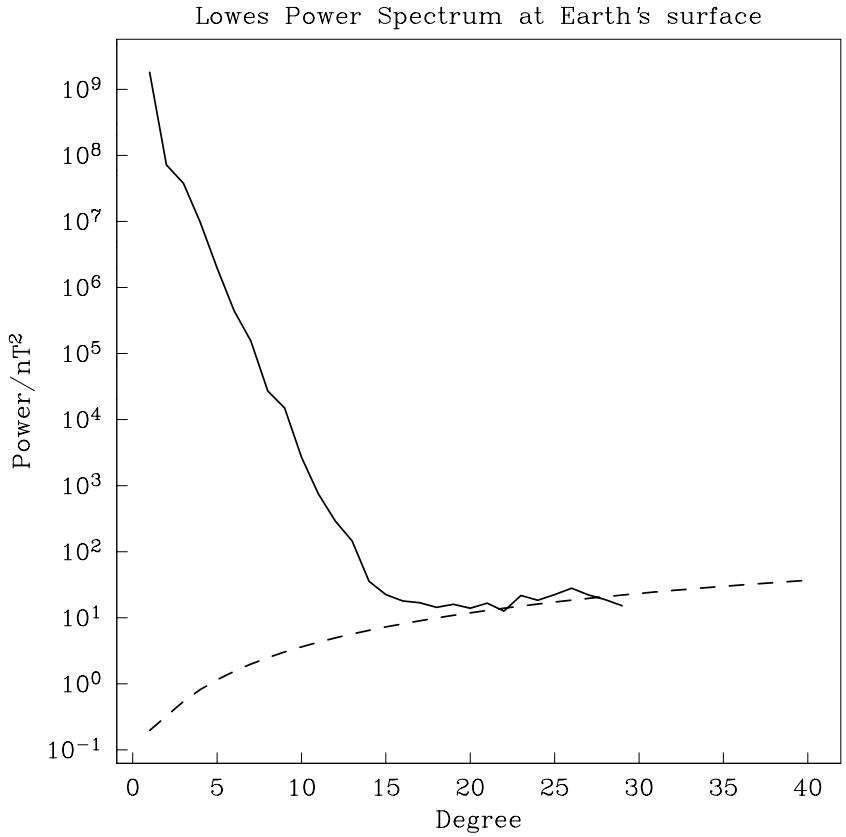

Figure 1. The geomagnetic power spectrum at the Earth's surface, often called the Lowes spectrum. It is accepted that degrees 1–14 represent the field from the core, largely unpolluted by the crustal magnetic field. Beyond degree 14 the signal is probably largely crustal in origin, and the power from the core is likely to be overwhelmed by this. In this region, the power spectrum forms a rigorous upper bound to the power from the core field. Also shown (dashed) is the spectrum predicted by model k_3 of Jackson (1994).

These values based on the magnetic field alone are quite small compared to the estimates of around 1–2 TW of Roberts *et al.* (2003) and of around 0.5 TW of Christensen & Tilgner (2004). A feature of variational problems is that the addition of extra constraints can never decrease the lower bound on the target function, and usually serve to increase the bound; therefore, ideally, one brings to bear on the problem as many constraints as is possible. Recently, Buffett *et al.* (2002) have used the observed nutations of the Earth to infer properties of the magnetic field at the CMB and ICB that are otherwise invisible to observation. They note the mismatch between the IAU 1980 nutation series and the observations, in particular, the out of phase component of the 18.6 yr retrograde nutation. This out of phase component argues for significant dissipation in the Earth, and Buffett *et al.*'s preferred explanation is in terms of electromagnetic coupling acting at the CMB and ICB. Their explanation of the observations does require a highly conducting lower mantle (in fact, with the same electrical conductivity as the core), and then determines the rms value of the radial magnetic fields on the surfaces of the inner and outer cores. The preferred values are $B_r(c)_{\rm rms} = 0.69$ mT and $B_r(b)_{\rm rms} = 7.1$ mT. Comparing the former value to the value inferred by observations of degrees 1–14 of the external field, namely 0.32 mT, we find that the extra power argues that the spectrum of B_r cannot drop off very quickly, indeed, it may remain flat out to high spherical harmonic degree, or even rise. This need for extra power in spherical harmonic degrees beyond the observable degrees 1–14 was demonstrated earlier by Buffett (1992), who showed that adopting a conducting layer at the base of the mantle with conductivity the same as that of the core could explain the nutation discrepancy if there was four times the energy in the radial field beyond degree 12 as was contained in the first 12 degrees. This meant $B_r(c)_{\rm rms}$ over all degrees was 0.67 mT, in accordance with the later results. We note that a recent study by Koot *et al.* (2008) has a value for the imaginary part of the ICB coupling constant which is at variance (by a factor of two) with the value used by Buffett *et al.* (2002); it is therefore possible that the value of the ICB field used here is not completely secure.

Observed values for $\langle B_r(r)^2\rangle$ provide constraints on any model of the magnetic field in the core, and can therefore be used to further refine the class of permissible models in the variational calculation. It is the use of these constraints that are the central thrust of this paper, and we use them to compute the minimum compatible Ohmic heating in the core. Indeed, a number of different calculations can be performed, using different combinations of (a) the observed Gauss coefficients β_l^m from degrees 1–14, (b) $\langle B_r(c)^2\rangle$ and (c) $\langle B_r(b)^2\rangle$. These calculations are presented in Sections 4 and 5.

The role of the magnetic field in the energetics of the core was first identified in Backus (1975) and Hewitt *et al.* (1975). These works note that it is actually the entropy increase associated with the Ohmic decay of the field that is the crucial quantity for driving the dynamo—in

other words, one must consider the entropy E_Φ, where

$$E_\Phi = \frac{1}{\sigma}\int \frac{\mathbf{J}^2}{\Theta}\,\mathrm{d}V \tag{7}$$

and Θ is the absolute temperature. Although the temperature of the core is subject to some debate, it is likely that it varies by only of the order of 25 per cent over its entire depth. Therefore, little error is incurred if temperature is taken outside the integral and E_Φ is set to Φ/T_{av} with T_{av} being the average temperature of the core. In this respect, the dissipation Φ remains a very central quantity, even if it is not strictly the entropy. Nevertheless, given an adiabatic profile for the core, one can readily calculate bounds on E_Φ in a similar fashion to Φ.

The arrangement of the paper is as follows: In Section 2, we introduce the poloidal–toroidal decomposition that is central to our analytical and numerical developments, and introduce the canonical form of the variational problem. In Section 3, we describe the form of the known solutions to the canonical P–G problem, including a treatment of the effect of imprecision in the observed values of the spherical harmonic decomposition of the magnetic field. In Section 4, we report on the solutions to a series of problems that only use the nutation constraints, but in various different combinations. Section 5 concerns itself with raising the bounds on dissipation higher by combining the nutation and magnetic field constraints. Some undesirable properties of the solutions found are avoided by the assignment of plausible but *ad hoc* spectral constraints in Section 6; the results for the dissipation reach values that are largely in accord with intuition, though these results cannot strictly be regarded as rigorous.

2 FORMULATION OF THE VARIATIONAL PROBLEM

We begin by setting up the general framework required for the subsequent calculations. We work entirely in terms of the magnetic field **B**, and the Ohmic heating, as defined by (1) is rewritten using the Maxwell equation $\nabla \wedge \mathbf{B} = \mu_0 \mathbf{J}$ as

$$\Phi = \frac{1}{\mu_0^2 \sigma}\int_V (\nabla \wedge \mathbf{B})^2\,\mathrm{d}V, \tag{8}$$

where μ_0 is the permeability of free space and V is the volume of the conducting spherical core. The core has constant electrical conductivity σ and outside the core the mantle is assumed to be an electrical insulator. We take the electrical diffusivity $\eta = (\mu_0\sigma)^{-1} = 1.6\,\mathrm{m^2\,s^{-1}}$, equivalent to a value for the conductivity of the core of $5 \times 10^5\ \mathrm{S\,m^{-1}}$.

The magnetic field in the core is decomposed using the Mie representation, which automatically ensures that the magnetic field is divergence free:

$$\mathbf{B} = \nabla \wedge \nabla \wedge (P\mathbf{r}) + \nabla \wedge (T\mathbf{r}). \tag{9}$$

The toroidal and poloidal scalars (T and P) are required to satisfy the boundary conditions on electric and magnetic fields across the interface between the core and the surrounding insulator. Although undoubtedly present in the core, the toroidal magnetic field has no radial component and thus does not enter into any calculation where poloidal (i.e. radial) fields are prescribed (Parker 1972; Gubbins 1975), and this remains true even for our calculations that involve rms values of the radial field determined from the nutation observations; thus only P will be important. The contribution of toroidal magnetic fields to the Ohmic heating remains unconstrained. The scalar P is expanded in terms of Schmidt quasi-normalized spherical harmonics with unknown radial functions $p_l^m(r)$. Matching to an exterior electrical insulator leads to a single boundary condition on the p_l^m of the form

$$\frac{\mathrm{d}p_l^m(r)}{\mathrm{d}r} + \frac{l+1}{r}p_l^m(r) = 0 \text{ at } r = c. \tag{10}$$

Following Backus *et al.* (1996), when (9) is inserted in (8), we find that the Ohmic heating can be written as

$$\Phi = -\frac{1}{\mu_0^2\sigma}\int \nabla^2 P\,\nabla^2\nabla_{\mathrm{h}}^2 P\,\mathrm{d}V, \tag{11}$$

where ∇_{h}^2 is the horizontal Laplacian. This then gives a total heat from the spherical harmonic expansion with degrees l and orders m of

$$\Phi = \sum_{l,m}\frac{4\pi l(l+1)}{\mu_0^2\sigma(2l+1)}\int_0^c r^2\left(\nabla^2 p_l^m(r)\right)^2\,\mathrm{d}r. \tag{12}$$

The minimum heating is a variational problem, solved by Gubbins (1975); when variations of (12) are taken, the resulting fourth-order differential equation has solutions of the form r^l, r^{l+2}, $r^{-(l+1)}$ and $r^{-(l-1)}$. When the whole sphere is considered, the finiteness of P dictates that the solution has no contribution from the two eigenfunctions that are singular there; two boundary conditions at the outer surface, one originating with matching the field to a vacuum field in the insulating exterior and the other stemming from the prescribed value of the field for a specific harmonic degree, complete the solution. We use the solution to this variational problem at several points in our analysis.

A useful facet of the problem is the absence of any dependence on angular order m in (12). This is a reflection of the rotational symmetry of the problem, and means that there is a degeneracy in order m, and all eigenfunctions of degree l are the same; this permits us to perform the calculation based only on the power per degree $\sum_m (\beta_l^m)^2$, rather than considering the spherical harmonic coefficients individually.

It is perhaps worth remarking on the similarity of variational problem (8) to two other similar variational problems. These allied problems are

$$\min \frac{\int_V (\nabla \wedge \mathbf{B})^2\,\mathrm{d}V}{\int_{V+\hat{V}} \mathbf{B}^2\,\mathrm{d}V}, \tag{13}$$

where $\hat{V}$ is the region of space outside V, and

$$\min \frac{\int_V (\nabla \wedge \mathbf{B})^2 \, \mathrm{d}V}{\int_V \mathbf{B}^2 \, \mathrm{d}V}. \tag{14}$$

These problems have been solved by Backus (1958) and Proctor (1977), respectively. The solutions of the first take the form of decay modes for the sphere (spherical Bessel functions), which are only slightly modified to become solutions of the second problem.

Returning to the variational problem at hand, namely (8), to perform numerical calculations we adopt a spectral representation of the poloidal scalar that has proven useful in other contexts: for each degree l and order m, we expand the radial functions $p_l^m(r)$ in terms of a Galerkin Chebychev basis $C_n(r)$, consisting of recombined Chebychev polynomials that automatically satisfy the boundary condition (10) (for details see Livermore & Jackson 2004):

$$p_l^m(r) = \sum_{n=0}^{N} {}^n p_l^m C_n(r). \tag{15}$$

The field is thus represented by coefficients $\{{}^n p_l^m\}$, where the index n signifies the radial basis function to which the coefficient is attached. The expansion terminates at $C_N(r)$ and thus there are $N + 1$ coefficients for each degree l and order m. These coefficients are stored in a model vector $\mathbf{m}$. We shall need expressions for the Ohmic dissipation and the value of the poloidal scalar at the CMB in this basis; they are respectively

$$\Phi = \mathbf{m}^T \mathbf{J} \mathbf{m} \tag{16}$$

and

$$p_l^m(c) = \mathbf{A}\mathbf{m}, \tag{17}$$

for given matrices $\mathbf{J}$ and $\mathbf{A}$.

3 THE CANONICAL P–G PROBLEM FOR OHMIC HEATING

The first calculations we perform are concerned with reproducing the results of Gubbins (1975) using our spectral basis: we have the bound (6) with which to compare. Given spherical harmonic coefficients $\{g_l^m; h_l^m\}$ to degree L, we have $D = L(L + 2)$ boundary values for the magnetic field poloidal scalar P; the problem then is to minimize Φ given by (16) subject to the D constraints

$$p_l^m(c) = a \frac{\beta_l^m}{l} \left(\frac{a}{c} \right)^{l+1}. \tag{18}$$

In our numerical implementation of the variational problem, we use the spectral expansion (15). To allow full generality of the problem, we actually impose the constraints (18) using two methods: in one we incorporate the linear constraints exactly, reducing the number of radial degrees of freedom of (15) by one for each degree l and in the other we use a quadratic penalty function. These two methodologies give us the flexibility to impose the constraints exactly, or to acknowledge that they are in fact imprecise measured values with associated errors and that they should be fit in a statistical sense, using their given error estimates. This latter scenario leads to the penalized least-squares problem amply described in Parker (1994). The problem becomes to minimize

$$\mathbf{m}^T \mathbf{J} \mathbf{m} + \lambda \left[\mathbf{A}\mathbf{m} - \mathbf{c} \right]^T \mathbf{C}_\mathrm{e}^{-1} \left[\mathbf{A}\mathbf{m} - \mathbf{c} \right], \tag{19}$$

where $\mathbf{C}_\mathrm{e}$ is the covariance matrix of the errors on the β_l^m (taken to be diagonal), $\mathbf{c}$ stores the observed values on the right-hand side of (18) and λ is chosen to attain a suitable misfit to the data, chosen so that

$$\frac{1}{D} \left[\mathbf{A}\mathbf{m} - \mathbf{c} \right]^T \mathbf{C}_\mathrm{e}^{-1} \left[\mathbf{A}\mathbf{m} - \mathbf{c} \right] = 1. \tag{20}$$

We perform two calculations, one treating the measured β_l^m as exact (the canonical P–G problem) and the other treating them as imprecise, to illustrate the effect of errors on the measurements.

The errors on the Gauss coefficients $\{\beta_l^m\}$ that enter $\mathbf{C}_\mathrm{e}$ are taken from the crustal model of Jackson (1994). This model predicts the power that lies in the crustal field at all spherical harmonic degrees, based on a stochastic model for the magnetization of the crust. It predicts larger, and more realistic errors, than would be given by the *a posteriori* covariance matrix that results from a spherical harmonic model of the field. These formal errors from the least-squares fitting procedure do not acknowledge that the field in degrees 1–14 has contributions from both core and crust. Therefore, one needs to adopt a measure of the probable contamination of the measured $\{\beta_l^m\}$ by the crust. We adopt the model k_3 with parameters $\nu = 0.995$ and $k(\beta) = 6$ (see Jackson 1994), since this predicts larger errors than does model k_4. Fig. 1 shows the k_3 spectrum from which these errors are calculated.

Fig. 2 shows the radial eigenfunctions for the first eight spherical harmonic degrees. The known eigenfunctions for this problem take the form

$$p_l^m(r) = c \left[-\frac{2l+3}{2l} \left(\frac{r}{c} \right)^l + \frac{2l+1}{2l} \left(\frac{r}{c} \right)^{l+2} \right] \beta_l^m, \tag{21}$$

(see Backus *et al.* 1996). The Ohmic dissipation as a function of position is plotted in Fig. 3 as the truncation level is raised from degree 1 to 2 and finally to 14. One can see that the highest dissipation tends to be close to the CMB. In terms of dynamo thermodynamic efficiencies, it

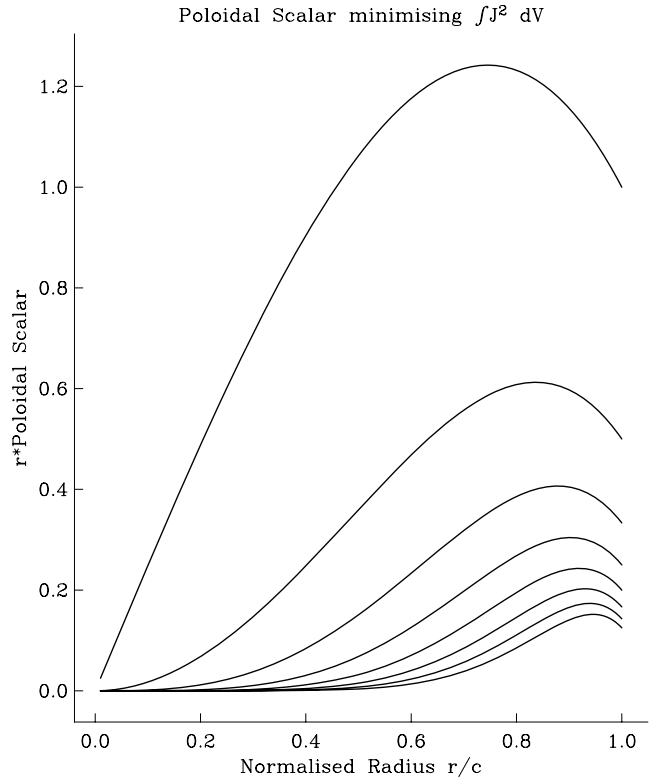

Figure 2. Behaviour of the poloidal scalar times radius for the minimum dissipation problem, when only observed values of the β_l^m on the CMB are prescribed (Gubbins 1975). The amplitude is arbitrary, though the largest in the figure corresponds to $l = 1$ and the smallest to $l = 8$.

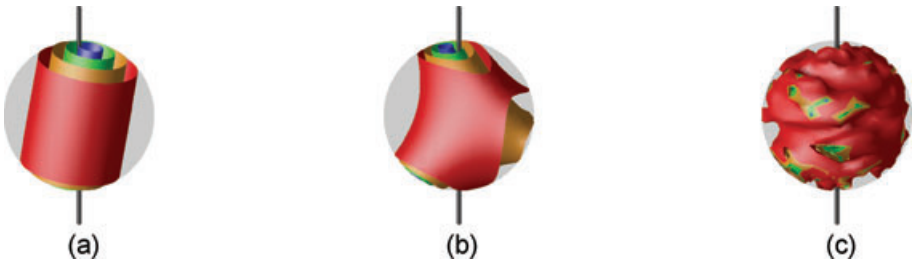

Figure 3. Isosurfaces of $|\mathbf{J}|^2$ for the canonical P–G problem for (a) $L = 1$, (b) $L = 2$ and (c) $L = 14$. In all cases, the red isosurface is that with the highest squared current density. Note that the highest local dissipation tends to be close to the CMB.

is perhaps worth remarking that this is a disadvantageous situation, indeed it would be much better if more of the heat were generated close to the ICB where the temperature is higher, leading to a higher Carnot efficiency factor. We shall see that some of our solutions have this property.

In terms of results for total dissipation, when the constraints are fit exactly we find $\Phi_{\min} = 2.93 \times 10^8$ W (agreeing with the value below eq. 6), and when they are fit weighted inversely with their errors using the criterion (20) we find $\Phi = 2.91 \times 10^8$ W, a trivial difference.

4 CALCULATIONS WITH QUADRATIC NUTATION CONSTRAINTS

We wish to introduce the constraints on the field behaviour in the core based on the considerations of the nutations of the Earth described by Buffett *et al.* (2002). As a result, we now perform the calculation of minimizing the Ohmic heating when mean-square radial field strengths are prescribed on the CMB and ICB. We refer to the constraints of squared radial field on the CMB and ICB as C_1 and C_2. The constraints can be written

$$C_1 = \sum_{l,m} \int \left[\frac{l(l+1)}{c} p_l^m(c) Y_l^m(\theta, \phi) \right]^2 \mathrm{d}\Omega = \frac{4\pi}{c^2} \sum_l \frac{l^2(l+1)^2}{2l+1} \sum_m p_l^m(c)^2, \tag{22}$$

$$C_2 = \sum_{l,m} \int \left[\frac{l(l+1)}{b} p_l^m(b) Y_l^m(\theta, \phi) \right]^2 \mathrm{d}\Omega = \frac{4\pi}{b^2} \sum_l \frac{l^2(l+1)^2}{2l+1} \sum_m p_l^m(b)^2. \tag{23}$$

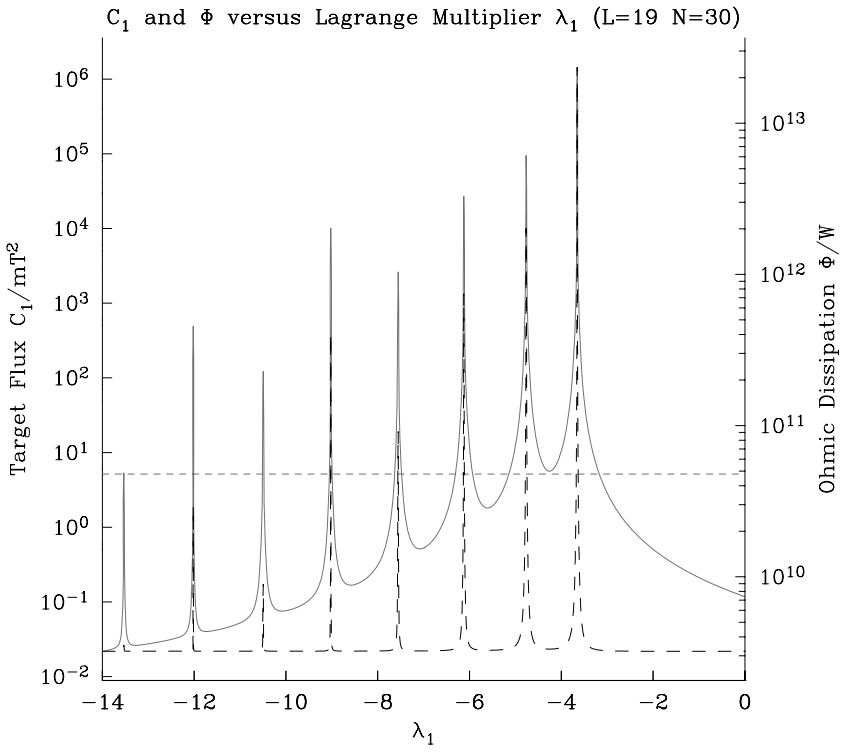

Figure 4. Example of the method for determining the correct Lagrange multiplier λ_1. This is for the example $L_{\min} = 2$, $L = 19$, $N = 30$ and upper bounds prescribed for the β_l^m for $l = 15$–19. Computations are performed for a series of values of λ_1, determining the correct λ_2 at each one. In green is the value of $\langle B_r(c)\rangle$ with the target value as a dashed horizontal line (left-hand scale). The dashed line corresponds to the Ohmic heating (right-hand scale). Of the many intersections of the green line with the target, only one has the minimum associated Ohmic heating (the largest λ_1). The value of λ_1 that minimizes the Ohmic dissipation in this case is -3.6.

The following sections explain a series of implementations of the constraints; we firstly describe the numerical implementation of the constraints using the spectral basis (15). This is important because the ultimate problem we wish to solve, which embraces all the constraints in the form of both (10) and (18) and of (22) and (23) can only be solved numerically. The problem with only constraints (22) and (23) has analytical solutions as we shall see.

4.1 Quadratic constraints: numerical implementation

The problem of minimizing (12) subject to (10), (22) and (23) is independent of order m and so it is only the total power per degree that is of importance, which can be implemented without loss of generality as axisymmetric harmonics. It is not clear that the solution separates in l as is the case for the canonical P–G problem, so one solves simultaneously for L radial expansions $p_l^0(r)$. Using the spectral basis (15), the values of C_1 and C_2 can be written in terms of the model as

$$C_1 = \mathbf{m}^T \mathbf{C_1} \mathbf{m}, \; C_2 = \mathbf{m}^T \mathbf{C_2} \mathbf{m}, \tag{24}$$

where $\mathbf{m}$ contains $L(N+1)$ parameters. Note the notational distinction between the target value of the constraint, C_1, and the matrix which defines the norm of the model, $\mathbf{C_1}$. We form the constrained functional

$$\mathbf{m}^T \mathbf{J} \mathbf{m} + \lambda_1 \left[\mathbf{m}^T \mathbf{C_1} \mathbf{m} - C_1\right] + \lambda_2 \left[\mathbf{m}^T \mathbf{C_2} \mathbf{m} - C_2\right], \tag{25}$$

using Lagrange multipliers λ_1 and λ_2. The minimum of this is clearly when

$$\mathbf{J}\mathbf{m} + \lambda_1 \mathbf{C_1}\mathbf{m} + \lambda_2 \mathbf{C_2}\mathbf{m} = 0. \tag{26}$$

To find the correct values of λ_1 and λ_2 such that the constraints are satisfied exactly, we first set λ_1 to a known value. We then discover the correct value of λ_2 by solving the generalized eigenvalue problem

$$\left[\mathbf{J} + \lambda_1 \mathbf{C_1}\right] \mathbf{m} = -\lambda_2 \mathbf{C_2} \mathbf{m} \tag{27}$$

for the $(N+1)L$ eigenvalues λ_2. The most positive eigenvalue is the one of interest, since it leads to the minimum Ohmic dissipation. We now scan through different values of λ_1, solving the eigenvalue problem at each value to find the appropriate λ_2. Fig. 4 shows the multiple values of λ_1 that fit the constraint. Again, the most positive one is the appropriate choice. We can also solve the similar problem when only one constraint is imposed, though in this case the problem can be solved as an eigenvalue problem without the need for a line search. All the solutions turn out to be single l solutions, a fact that can be seen from the block diagonal structure of the matrices $\mathbf{J}$, $\mathbf{C_1}$ and $\mathbf{C_2}$.

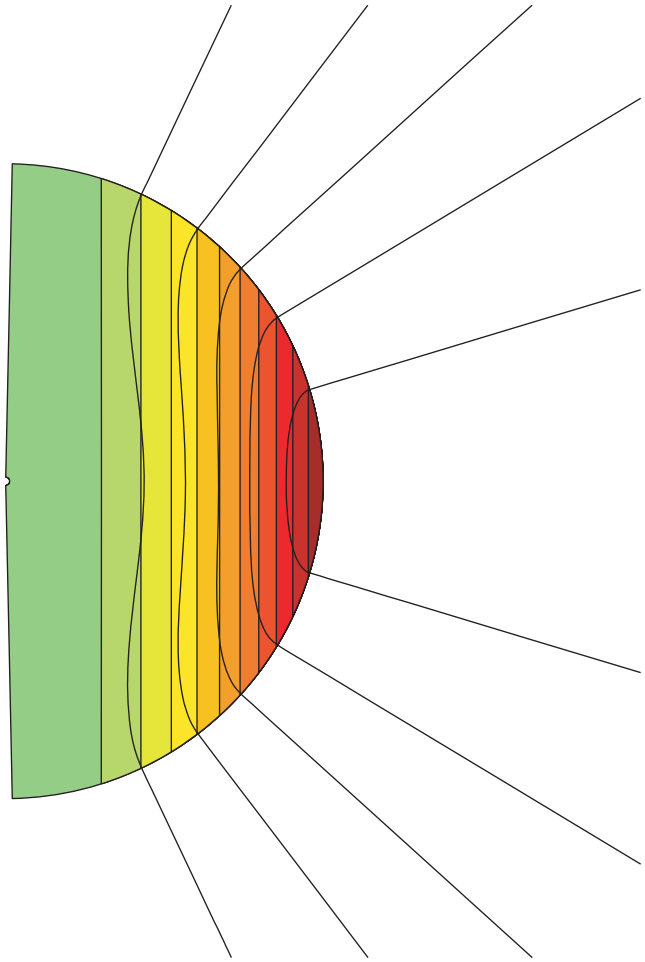

Figure 5. Field lines and current density shown for the $l = 1$ canonical P–G solution. Green colours are low current density and red colours are high current density.

The problem of minimizing the Ohmic dissipation subject to known rms radial field on the CMB has a solution that is exactly the $l = 1$ canonical P–G solution. However, the dissipation associated with the solution is now 5.97×10^8 W, 10 times higher than the $l = 1$ value for the Parker (1972) problem as a consequence of the higher value of the rms field at the CMB demanded by the nutation observations. Because we have told the variational problem nothing other than the rms field strength, the solution found is degree 1 despite the fact that we know that most of the power for the true Earth must be beyond the observable range of degrees 1–14. This deficiency will be addressed in Section 5. In Fig. 5, we show the current density in the core associated with this solution: it is a toroidal current growing linearly with cylindrical radius s, of the form (see Parker 1972)

$$\mathbf{J} = \frac{15r\sin\theta}{\mu_0 c^2}\beta_1^0\,\hat{\phi} = \frac{15s}{\mu_0 c^2}\beta_1^0\,\hat{\boldsymbol{\phi}}, \tag{28}$$

where $\hat{\boldsymbol{\phi}}$ is the unit vector in the azimuthal direction.

Table 2 shows the results of imposing the constraints separately and jointly. We make use of the fact that Buffett *et al.* (2002) are able to decompose the radial field power that they require into a dipole contribution and a uniform field contribution which we take to be the contributions from degrees higher than 1 (see Table 1). This means that we can divide the problems into degree 1 contributions (i.e. by solving with only degree 1 allowed) and a problem where degree 1 is not in the solution space (i.e. by solving with only spherical harmonics between 2 and L allowed). By this mechanism, the figure given above for the minimum dissipation solution subject to $\langle B_r(c)\rangle$, namely 5.97×10^8 W, is raised to 7.23×10^8 W.

If one were not to impose this division and simply implemented either of C_1 or C_2, the optimizing field is entirely $l = 1$. For the case where both constraints C_1 and C_2 are imposed Fig. 6 shows the poloidal scalar that achieves the minimum Φ. This is an entirely $l = 1$ solution. When one implements the division between $l = 1$ and $l > 1$ given in Table 1, one obtains the results of Table 2. The total dissipation associated with this case is 8.56×10^9 W, approaching 30 times larger than the value for the canonical P–G problem.

Table 1. The field strengths in mT determined by Buffett *et al.* (2002).

	$l = 1$	$l > 1$	Total
CMB rms field: $B_r(c)_{\rm rms}$ (mT)	0.212[a]	0.640	0.674
ICB rms field: $B_r(b)_{\rm rms}$ (mT)	4.33	5.72	7.17

Note: These give the ratio $\alpha = 0.049$ (defined below eq. (36) for the dipole, and $\alpha = 0.115$ for the rest.
[a]The value has been changed from that quoted by Buffett *et al.* (2002). They use the values given by Langel & Estes (1982) and deduce that the dipole field has an rms value of 0.264 mT, but this answer is in error by a factor of $\sqrt{3/2}$, and consequently we have changed it to the correct value of 0.212 mT. See also Mathews & Guo (2005).

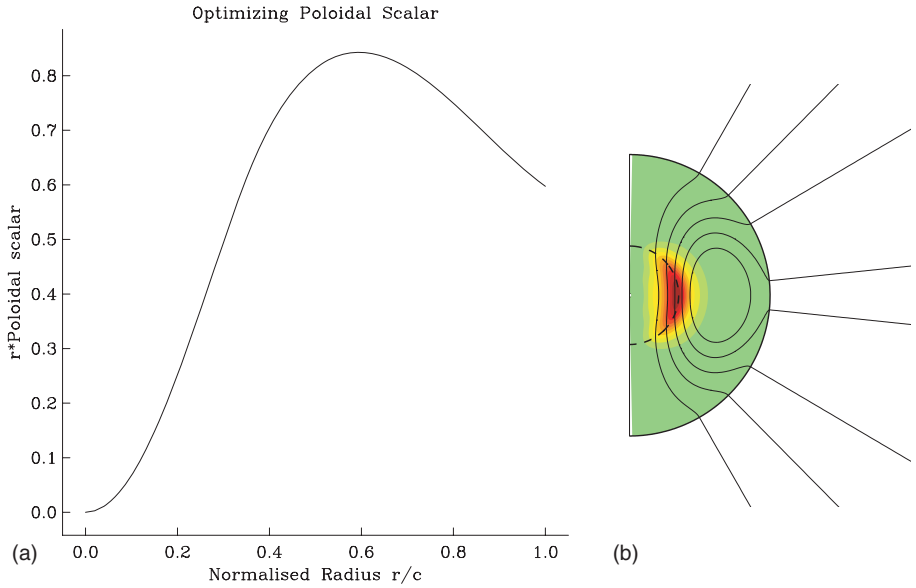

Figure 6. Characteristics of the solution when constraints C_1 and C_2 are implemented ($l = 1$ mode). (a) Poloidal scalar times radius as a function of radius. (b) Contours of $\mathbf{J}^2$ and field lines when the solution is assumed to be axisymmetric. The dashed line indicates $r = b$.

4.2 Known rms radial field strength on the ICB and CMB: analytical solution

If we consider the problem of minimizing the Ohmic heating when just the rms values of B_r are given on $r = c$ and $r = b$, the solution can be found analytically. We know from the structure of the problem described in Section 4.1 that the solution is a single harmonic degree l, with no mixing; however, the question remains, which l gives the minimum? We begin by dividing the core into two regions, labelled I and II in Fig. 7, corresponding to the inner and the outer cores, respectively. Since in regions I and II the solution minimizes the dissipation, we can make use of the linear combination of eigenfunctions that solve the variational problem defined by minimizing the squared current density throughout the core (Gubbins 1975; Backus *et al.* 1996). In region I, we write

$$P = \sum A_l r^l + B_l r^{l+2}, \tag{29}$$

where we have explicitly excluded the eigenfunctions that are singular at the origin. In region II, we write

$$P = \sum C_l r^l + D_l r^{l+2} + E_l r^{-(l+1)} + F_l r^{-(l-1)}. \tag{30}$$

Table 2. Heating in Watts due to different combinations of the quadratic nutation constraints.

	Dissipation Φ (W)		
Constraint applied	$l = 1$	$l > 1$	Total
$\langle B_r(c)^2 \rangle$	5.64×10^7	6.66×10^8	7.23×10^8
$\langle B_r(b)^2 \rangle$	1.94×10^9	5.76×10^9	7.70×10^9
$\langle B_r(c)^2 \rangle$ & $\langle B_r(c)^2 \rangle$	2.78×10^9	5.77×10^9	8.56×10^9

Note: We use the values of Table 1 for the field strengths.

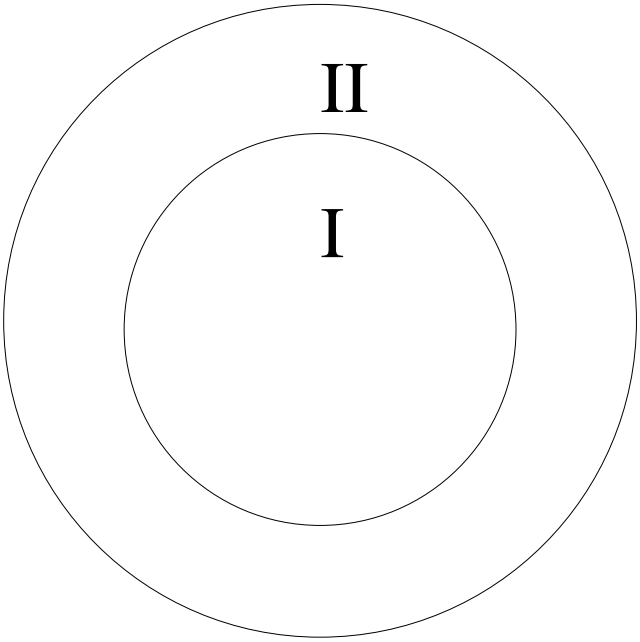

Figure 7. The regions I and II, corresponding to the inner and the outer cores, respectively, used for the boundary value problem of Section 4.

At the boundaries between I and II, and also at the boundary between II and the mantle, we impose continuity of the poloidal scalar P and its derivative P' to the potential field outside, which has known amplitude. Hence, we have at the ICB where $r = b$

$$A_l b^l + B_l b^{l+2} = C_l b^l + D_l b^{l+2} + E_l b^{-(l+1)} + F_l b^{-(l-1)}, \tag{31}$$

$$A_l l b^{l-1} + B_l (l+2) b^{l+1} = C_l l b^{l-1} + D_l (l+2) b^{l+1} - E_l (l+1) b^{-(l+2)} - F_l (l-1) b^{-l}, \tag{32}$$

and at the CMB we have

$$C_l c^l + D_l c^{l+2} + E_l c^{-(l+1)} + F_l c^{-(l-1)} = -c B_r(c)/(l(l+1)), \tag{33}$$

$$C_l l c^{l-1} + D_l (l+2) c^{l+1} - E_l (l+1) c^{-(l+2)} - F_l (l-1) c^{-l} = B_r(c)/l, \tag{34}$$

where $B_r(c)$ is the radial field in the lth harmonic degree, and we will assign all $(2l + 1)$ harmonics to have the same power in the ultimate solution that uses the rms values on c and b. At the ICB, we define the amplitude of the field, so that

$$A_l b^l + B_l b^{l+2} = -b \frac{B_r(b)}{l(l+1)}. \tag{35}$$

There are thus five equations in six unknowns, and hence the solution can be written with one free parameter. The Ohmic heating is then optimized as a function of that parameter by discovering the stationary value of the resulting quadratic; when this occurs the Ohmic heating is found to be

$$\begin{aligned} \Phi = & \frac{16\pi c \eta B_r(r_i)^2 (2l+3)(2l+1)}{\mu_0} \\ & \times \frac{\left\{\alpha(2l-1)\left[r_i^2 + 2l\left(r_i^2 - 1\right) - 3\right] r_i^{l+1} + (2l-1) r_i^2 + \alpha^2 \left[(4l+2) r_i - (2l+3) r_i^{2l}\right]\right\}}{l(l+1)\left[8 r_i - (4l^2 + 8l + 3) r_i^{2l} + (8l^2 + 8l - 6) r_i^{2l+2} - (4l^2 - 1) r_i^{2l+4}\right]}, \end{aligned} \tag{36}$$

where $\alpha = B_r(c)/B_r(b)$ is the fractional field strength at the core surface compared to that at the ICB; and $r_i = b/c$ is the radius of the inner core measured as a fraction of the outer core radius. Asymptotically, at large l, the dissipation increases linearly with l.

4.3 Known rms radial field strength on the ICB: analytical solution

In a similar vein to the above calculation, one can solve exactly for the poloidal scalar that minimizes the Ohmic dissipation when the rms radial magnetic field is given only on the ICB. In this case, we find the inner and outer solutions (in regions I and II) take the single-l form

$$p_l^m(r) = \begin{cases} B_r(b) \left(\frac{r}{b}\right)^l \frac{\left[\left(4l^2-1\right) r^2 - (2l+3) b \left(-2b^{2l} + 2lb + b\right)\right]}{2l(l+1)\left[(2l+3) b^{2l} - 2(2l+1) b\right]} & r \le b \\ B_r(b) \left(\frac{b}{r}\right)^{l+1} \frac{\left[(4l+6) r^{2l+1} - \left(4l^2+8l+3\right) r^2 \left(4l^2-1\right) b^2\right]}{2l(l+1)\left[(2l+3) b^{2l} - 2(2l+1) b\right]} & r \ge b \end{cases}, \tag{37}$$

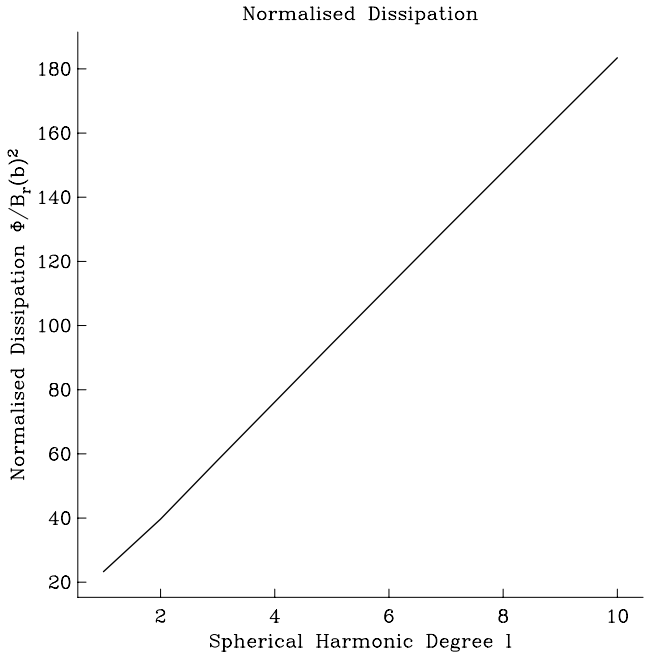

Figure 8. Minimum dissipation as a function of l for the problem where $B_r(b)$ is prescribed. The solution is normalized by the value of $B_r(b)^2$.

where $B_r(b)$ is the field equally distributed in one of the $(2l+1)$ modes of degree l, and the minimum heating is

$$\Phi_l = \frac{\eta}{\mu_0} 4\pi b^2 B_r(b)^2 \frac{(2l+1)^2\left(4l^2+4l-3\right)}{l(l+1)\left[(4l+2)b-(2l+3)b^{2l}\right]}. \tag{38}$$

In Fig. 8, we see that the contribution rises monotonically with l (a fact deducible from the asymptotics of 38), showing that the minimum is obtained when $l = 1$ only, in agreement with intuition. When $l = 1$ the minimum dissipation is

$$\Phi = \frac{\eta}{\mu_0} \frac{90\pi b B_r(b)^2}{6-5b} \tag{39}$$

with a poloidal scalar given (for each of the three contributing $l = 1$ modes) by

$$P = \begin{cases} B_r(b)\left(\frac{r}{b}\right) \frac{\left[3r^2-5b\left(3b-2b^2\right)\right]}{4\left(5b^2-6b\right)} & r \le b \\ B_r(b)\left(\frac{b}{r}\right)^2 \frac{\left(10r^3-15r^2+3b^2\right)}{4\left(5b^2-6b\right)} & r \ge b \end{cases}. \tag{40}$$

This scalar is shown in Fig. 9. The fact that the numerical solution based on the recombined Chebychev expansion is everywhere differentiable whereas the analytical solution is not at $r = b$ appears to make little difference, since the actual values for the dissipation are indistinguishable.

5 COMBINED USE OF NUTATION AND GEOMAGNETIC CONSTRAINTS

In Section 4 we used the nutation constraints, but this left the observed field at the core surface undue freedom in the range $l = 1$–14 to adapt itself to minimize the net rms currents. In this section, we reimpose the constraints (18) to ensure that the low degree field is in accord with the observations.

The study of Buffett *et al.* (2002) was able to discriminate between the contribution to the rms radial magnetic field of $l = 1$ and the contribution from all the other harmonics at the CMB and ICB, see Table 1. For this reason, we carry out separate calculations for the $l = 1$ component and for the remaining components. These results are shown in Tables 2 and 4. The $l = 1$ calculations are particularly easy and are very similar to the calculations of the previous section. The total dissipation is simply the sum of these contributions.

To carry out the $l > 1$ calculations, we must remove the known contribution of degrees 2–14 to the integrated squared field at the CMB; this removes 0.76 mT^2 from the nominal value of 5.15 mT^2 (see Table 1) and thus we generate the constraint C_3 where

$$C_3 = \mathbf{m}^T \mathbf{C_3} \mathbf{m}. \tag{41}$$

The numerical value of C_3 is 4.39 mT^2 but this constraint is only pertinent to the degrees larger than 14. In view of the results of Section 3 we impose the constraints from degrees 1–14 exactly, whilst demanding that C_2 and C_3 are also fit. We find that this raises the Ohmic heating to 1.245×10^{10} W, and that the spherical harmonic spectrum at the CMB takes the form shown in Fig. 10: all of the power required to match constraint C_3 is now contained in degree 15. The CMB field is not allowed to have such a large degree 15 component, since it would be visible at the Earth's surface and would be much larger than the observed spectrum. Although we believe the power observed in the degrees

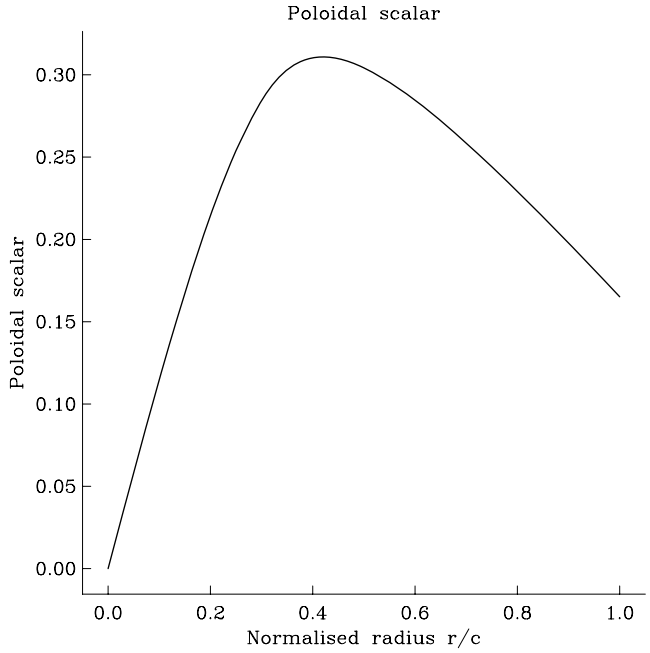

Figure 9. Poloidal scalar ($l = 1$) for the problem when the radial field is given on the ICB.

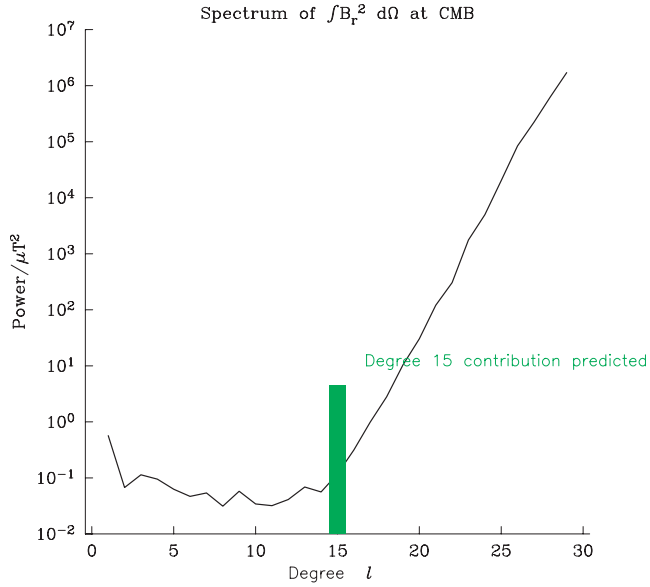

Figure 10. Plot of $\int B_r^2 \, \mathrm{d}\Omega$ at the CMB from model CO2. Also shown is the power predicted at degree 15 when the $\{\beta_l^m : 1 \leq l \leq 14\}$ are constrained along with C_1 and C_2, demonstrating that this power would exceed the power in the crustal field by a large amount.

from 15 onwards represents the crustal field and not the core field, we can make use of these values as 'upper bounds' on the core spectrum: it is a certainty that the core spectrum cannot exceed these values.

In fact the desire for the dissipation-minimizing solution to put all the power required to satisfy constraint C_3 in the lowest spherical harmonic degree that is unconstrained means that the inequality constraints (from the crustal field upper bound) are then actually satisfied as equality constraints. We find that the solution has power equal to the upper bounds (supplied from the crustal part of the spectrum) for $14 \leq l \leq 18$, and that degree 19 has a value required to make the total squared flux correct (see Table 3). The dissipation associated with this solution is 1.247×10^{10} W. This is the final rigorous lower bound that can be formally placed on the dissipation.

And yet this solution has many unsatisfactory features. It is extremely unlikely that the power spectrum at the core surface would be approximately flat in degrees 1–14 before dramatically rising. We provide the results of two final calculations, which are not formally lower bounds, but are indicative values that are much more in accord with geophysical intuition. Let us assume that the power spectrum at the core surface is flat all the way out from l = 15 to l = 58, with a power $\langle B_r(c)^2 \rangle_l = 0.1$ mT^2 (see Fig. 11). This idea for the power spectrum is similar in nature to the one explored by Buffett (1992). We impose this constraint on the variational problem and find that the dissipation now

Table 3. Values of $\langle B_r(c)^2\rangle_l$ from the model CO2 for epoch 2001 up to degree 14.

Degree	$\langle B_r(c)^2\rangle_l(\mathrm{mT}^2)$
1	5.667×10^{-1}
2	6.737×10^{-2}
3	1.136×10^{-1}
4	9.505×10^{-2}
5	6.284×10^{-2}
6	4.690×10^{-2}
7	5.394×10^{-2}
8	3.131×10^{-2}
9	5.779×10^{-2}
10	3.429×10^{-2}
11	3.196×10^{-2}
12	4.124×10^{-2}
13	6.887×10^{-2}
14	5.621×10^{-2}
15	1.178×10^{-1}
16	3.149×10^{-1}
17	9.900×10^{-1}
18	2.799×10^{0}
19	1.658×10^{-1}

Note: For 15–18, the values are upper bounds on the core spectrum, again supplied by the model CO2. For degree 19, the upper bound is created by reducing the true value of 1.04×10^{1} mT^2 to the value given to match the total rms radial field on the CMB with that given by Buffett *et al.* (2002).

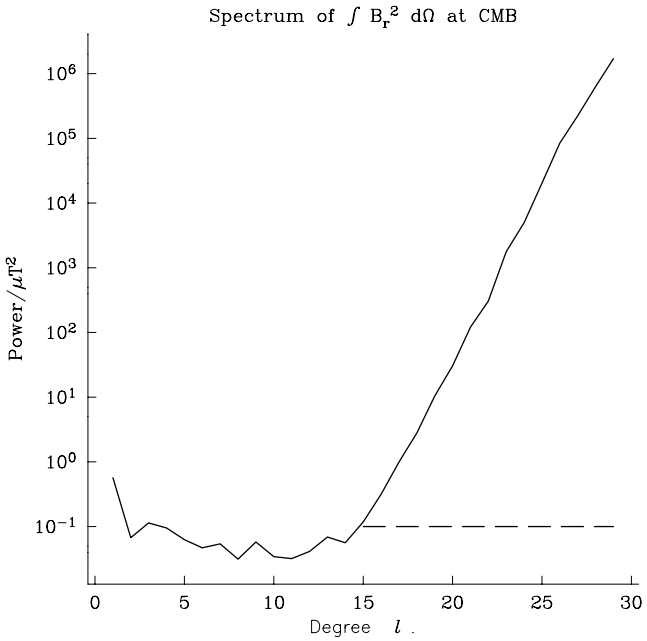

Figure 11. Plot of $\int B_r^2\,\mathrm{d}\Omega$ at the CMB from model CO2. Also shown is the flat spectrum assigned for $15 \leq 58$.

rises to 1.54×10^{10} W (see Table 4). Recall that we have split the $l = 1$ contribution out of these calculations because it can be solved for separately, as a result of the Buffett *et al.* (2002) rms field division given in Table 1. We briefly drop this division and use the total fields given in Table 1 in a calculation to illustrate one unsatisfactory feature of the solution to the flat spectrum problem. When we perform a calculation with all degrees l allowed, the problem is the fact that even though the solution at the CMB is a mixture of harmonics between degrees 1 and 58, the solution at the ICB is almost entirely degree 1. This is illustrated in Fig. 12 and occurs because the solution minimizes the dissipation by having most of the interior energy in the lowest degree. Of course the same behaviour occurs when we split off the $l = 1$ contribution, as we have usually done; in this case the field at the ICB is simply $l = 2$, the lowest degree available to the minimization. Although this solution satisfies all constraints applied to it, it falls short of geophysical reality. In the final spectrum, we investigate the effects of a more geophysically likely spectrum at the ICB.

Table 4. Minimum values for the Ohmic heating Φ when various constraints are applied to the problem.

Linear	Quadratic	Ohmic dissipation Φ (W)	Remarks
$l = 1$ only		5.66×10^7	Parker (1972) solution
$1 \le l \le 14$		2.93×10^8	Gubbins (1975) solution
$1 \le l \le 14$[a]		2.91×10^8	
	$\langle B_r(c)^2 \rangle$	7.23×10^8	*b, f*
	$\langle B_r(b)^2 \rangle$	7.70×10^9	*b, f*
	$\langle B_r(b)^2 \rangle$ and $\langle B_r(c)^2 \rangle$	8.56×10^9	*b, f*
$1 \le l \le 14$	$\langle B_r(b)^2 \rangle$ and $\langle B_r(c)^2 \rangle$	1.25×10^{10}	*f*
$1 \le l \le 19$[c]	$\langle B_r(b)^2 \rangle$ and $\langle B_r(c)^2 \rangle$	1.25×10^{10}	*f*
$1 \le l \le 58$[d]	$\langle B_r(b)^2 \rangle$ and $\langle B_r(c)^2 \rangle$	1.54×10^{10}	*f*
$1 \le l \le 58$[e]	$\langle B_r(b)^2 \rangle$ and $\langle B_r(c)^2 \rangle$	8.11×10^{10}	*f*

Note: In all cases the observed values for the Gauss coefficients β_l^m, supplying the linear constraints, are taken from the magnetic field model CO2 (Holme *et al.* 2003) for epoch 2001. The quadratic constraints come from Buffett *et al.* (2002). The diffusivity $\eta = 1.6$ throughout the paper. [a]Indicates that the Gauss coefficients are fit using their standard deviations and using a Chi-squared measure of misfit.
[b]Indicates that the solution would be purely $l = 1$ if only a total squared radial flux is supplied. In fact we split off the $l = 1$ solution as in Table 2, and solve for the remainder. This remainder solution is entirely $l = 2$.
[c]Indicates that the observed values of the crustal spectrum in CO2 are applied as upper bounds to the power in $15 \le l \le 19$ in the problem.
[d]Indicates that the values of $\langle B_r(c)^2 \rangle_l$ are set to $0.1\mu\ T^2$ for $15 \le l \le 58$ in the problem.
[e]Indicates that the values of $\langle B_r(c)^2 \rangle_l$ are set to $0.1\mu\ T^2$ for $15 \le l \le 58$ in the problem, and that $\langle B_r(b)^2 \rangle_l$ is also made to have the same spectrum as the CMB spectrum scaled by γ for $1 \le l \le 58$ (see eq. 42).
[f]Indicates that these problems have been solved by separating the $l = 1$ contribution from the rest, by using the division of the squared fields given in Table 1. Consequently, the problems are solved for the 'uniform field' contribution by performing the minimisation problems beginning with $l = 2$. The $l = 1$ solutions are exactly those of Table 2, and both $l = 1$ and $l > 1$ contributions are added to give the final value.

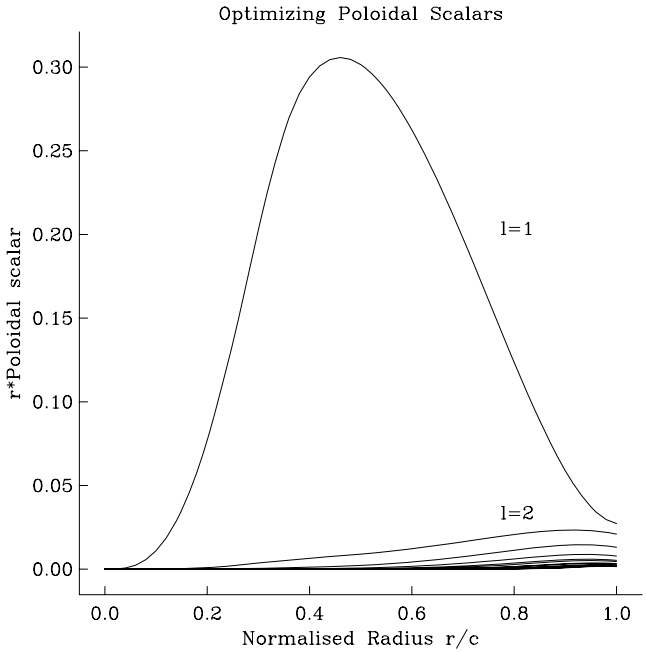

Figure 12. The optimizing poloidal scalars multiplied by radius as a function of normalized radius for the problem in which the entire spectrum $\{\langle B_r(c)^2 \rangle_l : 1 \le l \le 58\}$ is specified, along with $\langle B_r(b)^2 \rangle$; note that the $l = 1$ contribution is so much larger than the others.

6 ASSIGNMENT OF A PLAUSIBLE SPECTRUM AT THE ICB

Given a rich 'white' spectrum at the CMB, we believe it is contrary to intuition that the ICB spectrum would be dominated by a single low spherical harmonic degree. In this section, we extend the white spectrum assignment that we have applied to the CMB to the ICB by assigning each spherical harmonic degree to have a constant ratio between its values at the CMB and ICB. Since $\sqrt{\langle B_r(c)^2 \rangle_l / \langle B_r(b)^2 \rangle_l} = \gamma = 0.125$, we assign the ratio γ to be the ratio for every spherical harmonic degree. Thus, we have

$$\sqrt{\frac{\langle B_r(c)^2 \rangle_l}{\langle B_r(b)^2 \rangle_l}} = \gamma, \quad 1 \le l \le 58. \tag{42}$$

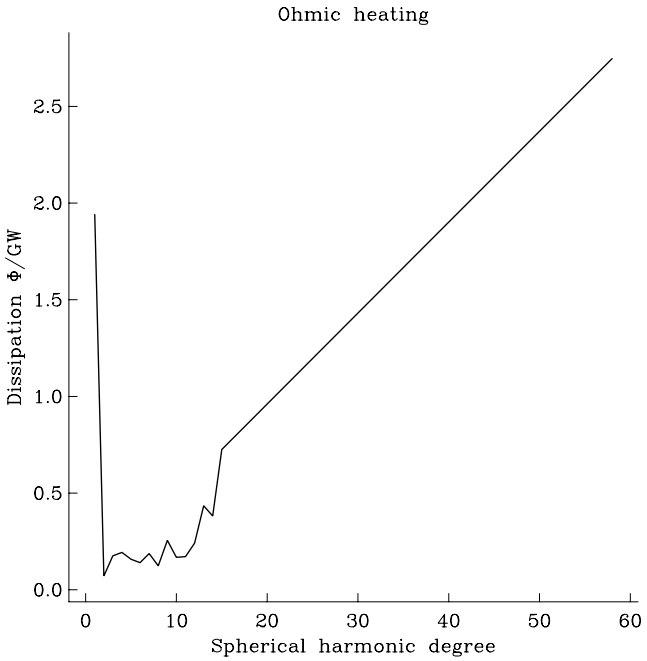

Figure 13. Ohmic heat as a function of spherical harmonic degree l for the final constrained problem in which the spectra at the CMB and ICB are constrained to be flat. Note the linear increase in the dissipation.

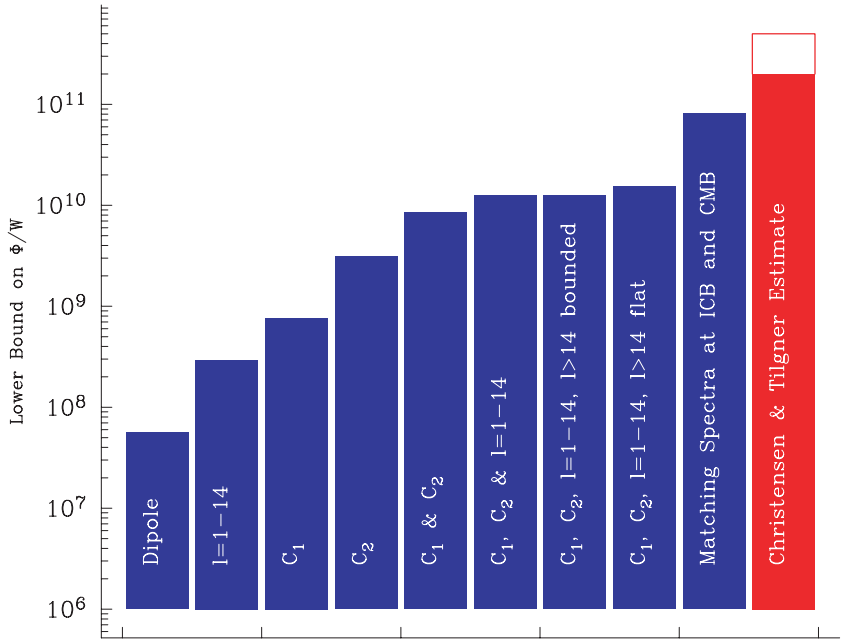

Figure 14. Bar chart showing how the different lower bound problems (blue) approach the estimate of Christensen & Tilgner (2004) (red) as different constraints are applied.

Since we now have constraints on every spherical harmonic degree, the solution now separates in l and we can find the value of the poloidal scalar for each degree l independently. This two-point boundary value problem is exactly that solved in Section 4. The Ohmic dissipation produced by each spherical harmonic degree is shown in Fig. 13. The total heating associated with this solution is 8×10^{10} W, within a factor of three of the 0.2–0.5 TW range for the dissipation found by Christensen & Tilgner (2004).

7 CONCLUSIONS

A variety of different constraints have been added to the canonical problem of Parker and Gubbins of minimizing the Ohmic dissipation in the core. All of the values for Ohmic heating are given in Table 4, and Fig. 14 shows pictorially how the imposition of different constraints leads

to a gradual sharpening of the lower bound, bringing it closer to the value of Christensen & Tilgner (2004). Applying geodetic observational constraints to the minimum Ohmic heating bound problem raises the lower bound by a factor of 30, from $\sim 3 \times 10^8$ W to almost 10 GW. This increase is completely dependent on the veracity of the interpretation of nutation mismatches between theory and observation being the result of electromagnetic coupling at the ICB and CMB. Although this is the formal minimum, it is unsatisfactory in many ways: the spectrum at the CMB is exactly that of the crustal spectrum, leaving no energy whatsoever for the crustal field in degrees 14–19; and additionally the spectrum at the ICB is almost entirely $l = 1$. These features are extremely unlikely in reality and therefore argue that the true minimum dissipation is still higher than this estimate. An *ad hoc* (and thus non-unique) method for moving the solution towards the geophysical regime is to assign the spectra of the radial field at the CMB and ICB. When these spectra are prescribed to be flat, the minimum dissipation rises to 0.08 TW. Although this is no longer a formal lower bound, we consider that it is a geophysically indicative number. This number is now within a factor of three of the value for the dissipation given by Christensen & Tilgner (2004), based on a suite of numerical dynamo runs.

The problem addressed in this paper ignores entirely the dynamics of the core. Because of the nature of the constraints, the solutions contain no toroidal field at all and consequently ignore any potential Ohmic dissipation associated with it. Since the toroidal field is thought to be strong in the Earth, this is a serious shortcoming. In the future, we will demonstrate how dynamical constraints can be incorporated into the variational problem that naturally contain toroidal field, raising the lower bound *en route* (without the need for *ad hoc* assumptions regarding the spectra at the ICB and CMB) and bringing the answers closer to geophysical reality.

ACKNOWLEDGMENTS

This paper is intended to honour the contributions made by David Gubbins up to his 60th birthday. Many of the calculations were performed when AJ was a visitor at IGPP, Scripps Institution of Oceanography, which he thanks for hospitality. We gratefully acknowledge the advice of Bob Parker regarding the solution of (26) and for the suggestion of setting the inner core spectrum to a more geophysically realistic form. This work has partly been supported by NSF grant 0724331.

REFERENCES

Backus, G., 1958. A class of self-sustaining dissipative spherical dynamos, *Ann. Phys.,* **4,** 372–447.

Backus, G.E., 1975. Gross thermodynamics of heat engines in deep interior of earth. *Proc. Natl. Acad. Sci. USA,* **72,** 1555–1558.

Backus, G., Parker, R. & Constable, C., 1996. *Foundations of Geomagnetism,* Cambridge Univeristy Press, Cambridge, UK.

Buffett, B.A., 1992. Constraints on magnetic energy and mantle conductivity from the forced nutations of the Earth, *J. geophys. Res.,* **97,** 19 581–19 597.

Buffett, B.A., Mathews, P.M. & Herring, T.A., 2002. Modeling of nutation and precession: effects of electromagnetic coupling, *J. geophys. Res.,* **107**(B4), doi:10.1029/2000JB000056.

Chapman, D.S. & Pollack, H.N., 1975. Global heat flow: a new look, *Earth planet. Sci. Lett.,* **28,** 23–32.

Christensen, U.R. & Tilgner, A., 2004. Power requirement of the geodynamo from Ohmic losses in numerical and laboratory dynamos, *Nature,* **429,** 169–171.

Davies, G.F., 1999. *Dynamic Earth—Plates, Plumes and Mantle Convection,* Cambridge University Press, Cambridge, UK.

Gubbins, D., 1975. Can the earth's magnetic field be sustained by core oscillations?, *Geophys. Res. Lett.,* **2,** 409–412.

Gubbins, D., Alfe, D., Masters, G., Price, D. & Gillan, M.J., 2003, Can the Earth's dynamo run on heat alone?, *Geophys. J. Int.,* **155,** 609–622.

Hewitt, J.M., McKenzie, D.P. & Weiss, N.O., 1975. Dissipative heating in convective flows, *J. Fluid Mech.,* **68,** 721–738.

Hernlund, J.W., Thomas, C. & Tackley, P.J., 2005. A doubling of the post-perovskite phase boundary and structure of the Earth's lowermost mantle, *Nature,* **434,** 882–886, doi:10.1038/nature03472.

Holme, R., Olsen, N., Rother, M. & Lühr, H., 2003. CO2: a CHAMP magnetic field model, in *Proceedings of the First CHAMP Science Meeting,* eds Reigber, Chr., Lühr, H. & Schwintzer, P., Springer Verlag, Berlin.

Iitaka, T., Hirose, K., Kawamura, K. & Murakami, M., 2004. The elasticity of the MgSiO3 post-perovskite phase in the Earth's lowermost mantle, *Nature,* **430,** 442–445.

Jackson, A., 1994. Statistical treatment of crustal magnetization, *Geophys. J. Int.,* **199,** 991–998.

Koot, L., Rivoldini, A., de Viron, O. & Dehant, V., 2008. Estimation of Earth interior parameters from a Bayesian inversion of VLBI nutation time series, *J. geophys. Res.,* **113,** B08414. doi:10.1029/2007JB005409.

Langel, R.A. & Estes, R.H., 1982. A geomagnetic field spectrum, *Geophys. Res. Lett.,* **90,** 2487–2494.

Lay, T., Hernlund, J., Garnero, E. & Thorne, M., 2006. A lens of post-perovskite and D″ heat flux beneath the central Pacific, *Science,* **314,** 1272–1276, doi:10.1126/science.1133280.

Lay, T., Hernlund, J.W. & Buffett, B.A., 2008. Core-mantle heat flow, *Nature Geosci.,* **1,** 25–32, doi:10.1038/ngeo.2007.44.

Livermore, P.W. & Jackson, A., 2004. On magnetic energy instability in stationary flows, *Proc. R. Soc.,* **460,** 1453–1476, doi:10.1098/rspa.2003.1200.

Mathews, P.M. & Guo, J.Y., 2005. Viscoelectromagnetic coupling in precession-nutation theory, *J. geophys. Res.,* **110,** B02402, doi:1029/2003JB002915.

McDonough, W.F. & Sun, S.-S., 1995. The composition of the Earth, *Chem. Geol.,* **120,** 223–253.

Montelli, R., Nolet, G., Dahlen, F.A., Masters, G., Engdahl, R.E. & Hung, S., 2004. Finite-frequency tomography reveals a variety of plumes in the mantle, *Science,* **303,** 338–343, doi:10.1126/science.1092485.

Murakami, M., Hirose, K., Kawamura, K., Sata, N. & Ohishi, Y., 2004. Post-perovskite phase transition in MgSiO3, *Science,* **304,** 855–858.

Nimmo, F., 2007. Thermal and chemical evolution of the core, in *Treatise on Geophysics,* Vol. 9, ed. Schubert, G., Elsevier, Amsterdam.

Oganov, A.R. & Ono, S., 2004. Theoretical and experimental evidence for a post-perovskite phase of MgSiO3 in Earth's D″ layer, *Nature,* **430,** 445–448.

Parker, R.L., 1972. Inverse theory with grossly inadequate data, *Geophys. J. R. astr. Soc.,* **29,** 123–138.

Parker, R.L., 1994. *Geophysical Inverse Theory,* Princeton Univeristy Press, Princeton, NJ.

Proctor, M.R.E., 1977. On Backus' necessary condition for dynamo action in a conducting sphere, *Geophys. astrophys. Fluid Dyn.,* **9,** 89–93.

Roberts, P.H., Jones, C.A. & Calderwood, A.R., 2003. Energy fluxes and Ohmic dissipation, in *Earth's Core and Lower Mantle,* pp. 100–129, eds Jones, C.A. & Soward, A. & Zhang, K. Taylor & Francis, London, UK.

Schubert, G., Turcotte, D.L. & Olson, P., 2001. *Mantle Convection in the Earth and Planets,* Cambridge Univeristy Press, Cambridge, UK.

Stieglitz, R. & Müller, U., 2001. Experimental demonstration of the homogeneous two-scale dynamo, *Phys. Fluids,* **13,** 561–564.